25th ABCM International Congress of Mechanical Engineering
October 20-25, 2019, Uberlândia, MG, Brazil

COB-2019-1574
INFLUENCE OF DIAMOND WIRE SAWING PARAMETERS ON SUBSURFACE MICROCRACKS FORMATION IN MONOCRYSTALLINE SILICON WAFER

Erick Cardoso Costa[1]
Caroline Piesanti dos Santos[2]
Fabio Antonio Xavier[3]
Walter Lindolfo Weingaertner[4]
Department of Mechanical Engineering, Precision Engineering Laboratory, Federal University of Santa Catarina, Florianópolis/SC, Brazil.
[1]erick.cardoso.costa@posgrad.ufsc.br
[2]caroline.piesanti@grad.ufsc.br
[3]f.xavier@ufsc.br
[4]w.l.weingaertner@ufsc.br

Abstract. *Multi-wire sawing is one of the machining processes for silicon wafer manufacturing. Although this process to be stable along the production chain, the knowledge about wafering process is still empirical, based mainly on operators' experience, trial and error. This is mainly due to machine-tool design complexity, material removal kinematic and silicon brittle behavior. Hence, the process still requires experimental investigations towards sawing process peculiarities. In this sense, the present paper aims to analyze cutting speed and feed speed influence on subsurface microcrack formation and surface roughness parameter R_z of monocrystalline silicon cut by endless diamond wire. Results showed that feed speed increase caused higher microcrack nucleation and propagation due to higher kinematic cutting edge penetration. On the other hand, increase of cutting speed promoted higher cutting edge engagement frequency, which decreased cutting edge penetration and led to smaller microcrack depth damage. In the same way, surface roughness parameter R_z was higher when feed speed enlarged and lower with wire cutting speed was larger. Both microcrack depth and surface roughness parameter R_z showed an upward linear correlation.*

Keywords: *endless diamond wire saw, monocrystalline silicon, subsurface microcrack damage, continuous sawing*

1. INTRODUCTION

Silicon crystal has been the dominant material for solar cells wafer manufacturing, detaining about 90% of photovoltaic market (LIU *et al*., 2017). In silicon wafers manufacture, Multi-Wire Sawing (MWS) is one of the main machining techniques employed in mass production and has been used since the 1990s (KLOCKE, 2009; LIU *et al*., 2017). The cutting process (see Fig. 1a) is based on feeding a single steel wire from a supply spool to a take-up spool. Wire is wrapped in parallel and equidistant grooves of guide cylinders, creating a wire web. Ingot is fed against the wire web and interaction between abrasives grains and silicon surface result in material removal. It promotes ingot slicing into hundreds or even thousands silicon wafers (WU, 2016).

MWS can be employ technologies with different kinematics of material removal mechanism, such as Multi-Wire Slurry Sawing (MWSS) and Diamond Wire Sawing (DWS). In the former (Fig. 1b), cut occurs using a slurry based on polyethylene glycol with silicon carbide (SiC) grains, which flows through nozzles onto the wire and then gets carried by it to the sawing channel. Interaction between SiC grains dispersed in the slurry and the silicon substrate define material removal mechanism, referred as three-body-wear. The other mechanism uses diamond abrasives grains electroplated with nickel in a steel wire (Fig. 1c). In this method, cut is performed by direct interaction of diamond grains with silicon substrate through two-body-wear (WU, 2016; MÖLLER, 2015).

Due to the higher material removal rate, lower subsurface depth damage, use of water-based coolant and better integrity surface, diamond wire sawing has been replacing wire slurry sawing. It is acknowledged that diamond wire sawing process have a great potential in substituting conventional sawing process. However, surface integrity damage on monocrystalline silicon (mono-Si), such as surface roughness, microcrack damage and phase transformation, are still unavoidable. At last, even though these sawing technologies has been employed for decades, few researches was performed until recent years.

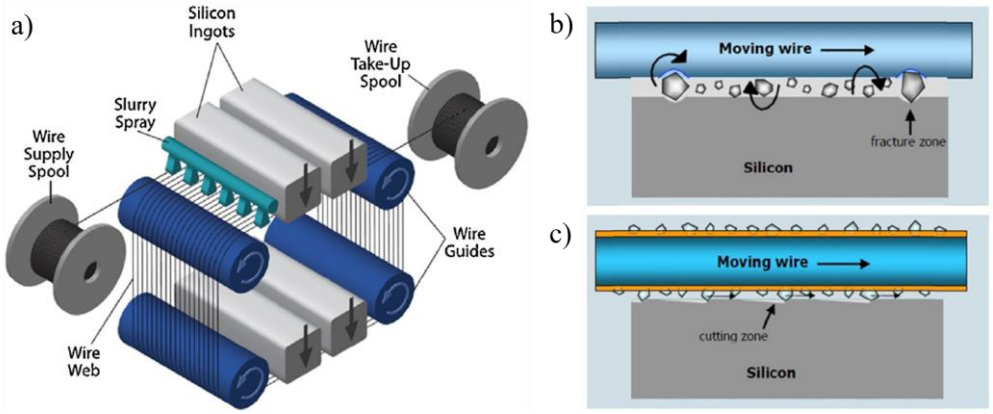

Figure 1. Multi-wire sawing process of silicon wafers: a) schematic of machine tool; b) wire slurry sawing; c) diamond wire sawing (WU, 2016).

Knowledge about wafering process is still empirical, based mainly on operators' experience, trial and error (KLOCKE, 2009). This is mainly due to the complexity of machine-tool design, material removal kinematics and silicon crystal brittle behavior. Even though silicon wafers machining process is stable along the production chain, its manufacturing costs represents about 50% of total solar cell fabrication cost (PEGUIRON *et al*., 2014). It means that the process still requires experimental investigations towards process optimization and a strategy found to decrease costs is to reduce wafer thickness. Currently, wafer thickness is around of 180 µm and one expects a further reduction down to 100 µm in some years.

Both time and removed material from subsequent silicon wafer processing (i.e. lapping, polishing, chemical removal) are directly proportional to subsurface microcracks depth, since they reduce significantly mechanical resistance, thus accelerating component breakage and decreasing solar cell lifetime (MÖLLER, 2015). According to the aforementioned, a deeper understanding of silicon wafers sawing process is an important subject to be investigated in order to reduce production costs and make solar energy more viable (COSTA *et al*., 2018). In this sense, the present paper aims to evaluate the influence of wire cutting speed (v_c) and feed speed (v_f) in mono-Si subsurface microcrack formation cut by an endless diamond wire sawing.

2. EXPERIMENTAL PROCEDURE

Experiments were performed using an endless wire saw test rig (see Fig. 2a) designed by Knoblauch (2019) by reconfiguring an ultra-precision machining system built by Stoeterau (1999). Product development process based on the Pahl and Beitz methodology (2007) was used and more information about the reconfiguration process can be found in the references Knoblauch (2019) and Knoblauch *et al*. (2017a). The test rig executes endless wire cutting movement through a continuous wire saw wrapped around Teflon pulleys (A and A' axis), where a three-phase electric motor powers the A axis and a frequency inverter is used to set the wire cutting speed (v_c) up to 26 m/s. A vertical aerostatic bearing (Y axis) moves the workpiece against the wire with feed speed $v_f \geq 0.08$ mm/min. Wire tension (T_{wire}) is set by air pressure control of a pneumatic cylinder (X axis) and the wafer thickness is adjusted in a screw (Z axis).

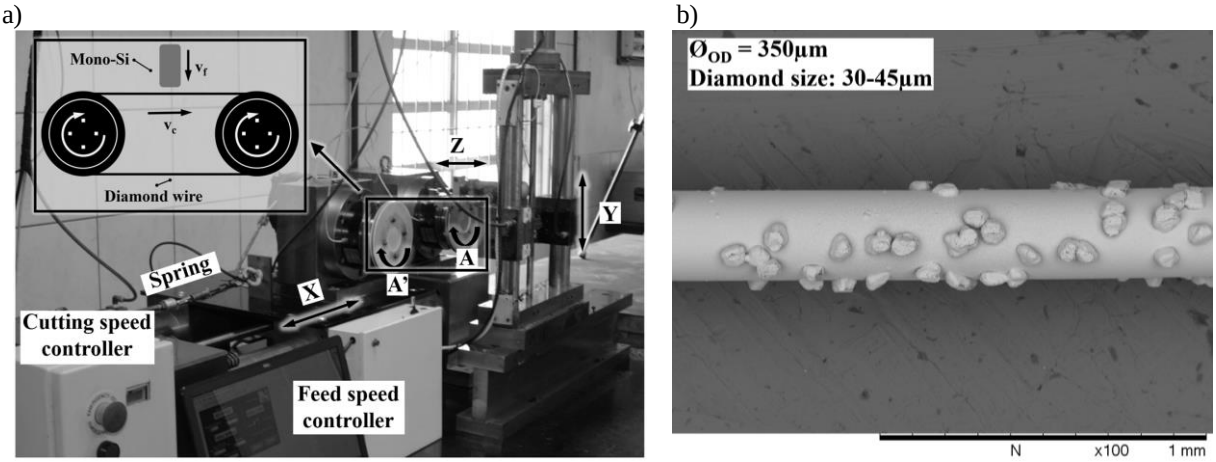

Figure 2. a) Endless wire saw test rig; b) SEM of electroplated diamond wire.

Cutting tool was an electroplated diamond wire with outer diameter of $Ø_{OD}$ = 350 µm (*Norton Saint-Gobain Abrasives Brasil*), as shown in Fig. 2b. For experiments, a 1m-length diamond wire segment was butt-welded into a loop using a diamond wire welding device developed for this purpose by Knoblauch *et al*. (2017b). Using looped diamond wire allows sawing with constant wire cutting and feed speed.

Specimens were rectangular blocks of monocrystalline silicon with dimensions 25 mm x 50 mm x 7 mm. The blocks were sawn into an average thickness of (1 ± 0.05) mm at the (100) crystallographic orientation, which was chosen due its wide use in solar cells production.

Trials were performed at different wire cutting speeds (10, 15 and 20 m/s) and feed speeds (20, 30 and 40 mm/min) and other parameters, i.e. diamond wire tension, were fixed (see Table 1). A 3^2 full factorial design of experiment (DOE) was applied to analyze factors effect, resulting in 9 tests. Two replicates were performed for each test, totalizing 27 trials. All cuts were executed dry and, in each cutting experiment, a new diamond wire saw was used.

Table 1. Design of experiments and sawing parameters

Test	**Conditions**		
	Wire cutting speed (v_c)	**Feed speed (v_f)**	**Wire tension (T_{wire})**
1	10 m/s	20 mm/min	20 N
2	10 m/s	30 mm/min	
3	10 m/s	40 mm/min	
4	15 m/s	20 mm/min	
5	15 m/s	30 mm/min	
6	15 m/s	40 mm/min	
7	20 m/s	20 mm/min	
8	20 m/s	30 mm/min	
9	20 m/s	40 mm/min	

Subsurface microcracks depth were analyzed using bevel-polishing method, as described by Tönshoff *et al*. (1997). Cold mounting was done with acrylic resin followed of metallographic procedure using sandpapers (220 to 2000 mesh) and slurry diamond abrasives polishing, with grain size of 0.25 µm. Afterward, samples were etched with Sirtl Etchant for 20s. Subsurface images were acquired by a Hitachi (TM-3030) scanning electron microscope (SEM). Average microcrack depth was calculated as described in ASTM F 950-02 standard.

To support analyzes of microcracks formation, surface topography was evaluated using a Taylor Hobson (FTS i120) profilometer, employing a diamond stylus tip with radius of 2 µm and cone angle of 90º. Surface roughness measurements were computed based on ISO 4288/1998 standards: 4 mm of sampling length and 0.8 mm cut-off. Mono-Si sawn profile was measured along feed direction and R_z parameter was extracted through data processing in MountainsMap Universal 7.1® software (ISO 4287/1997).

3. RESULTS

3.1 Microcrack damage depth

Residual damage in form of microcrack into subsurface was analyzed by SEM with bevel-polishing, as shown in the SEM image of monocrystalline silicon sawn subsurface in Fig. 3. Figure 4 shows microcracks depth average behavior under v_f and v_c variation. Microcrack depth revealed an average range between 5.6 and 8.4 µm, as expected by Möller (2015), which indicates that microcracks reaches depths between 2 and 20 µm into the subsurface.

In general, microcracks seen in Fig. 3 are generated mainly when mono-Si presents brittle behavior, as described by Lawn e Wilshaw (1975). Microcracks appearance are related to brittle fracture occurrence before material reaches plastic deformation during diamond grit cutting edge penetration. According to Bifano *et al*. (1991), for brittle and hard materials, there is a critical value ($h_{cu,crit}$) between plastic deformation and microcracks formation, where its extrapolation can be achieved by increasing cutting edge penetration. It promotes chip formation through microcrack, leading to microcracks initiation and propagation into the subsurface.

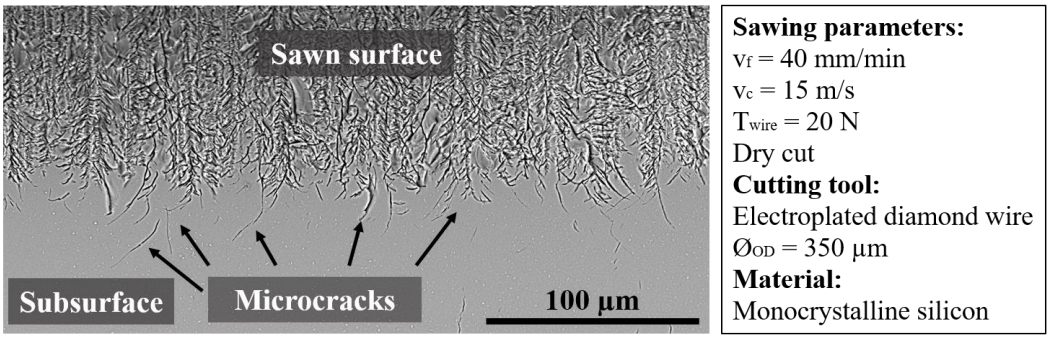

Figure 3. Subsurface microcrack damage of monocrystalline silicon cut by diamond wire sawing.

It is shown in Fig. 4 that microcracks have tended to increase when v_f increases from 20→30→40 mm/min. Examining microcrack growing behavior, according to Gao *et al.* (2016), microcracks depth increase occurs due to higher kinematic cutting edge penetration and force per grain (f_g) through cutting edge pressure against mono-Si surface. Thus, as stated by Klocke (2009), higher kinematic cutting edge penetration generates higher h_{cu}, enabling deeper microcracks initiation and propagation into the subsurface, as seen in Fig. 4.

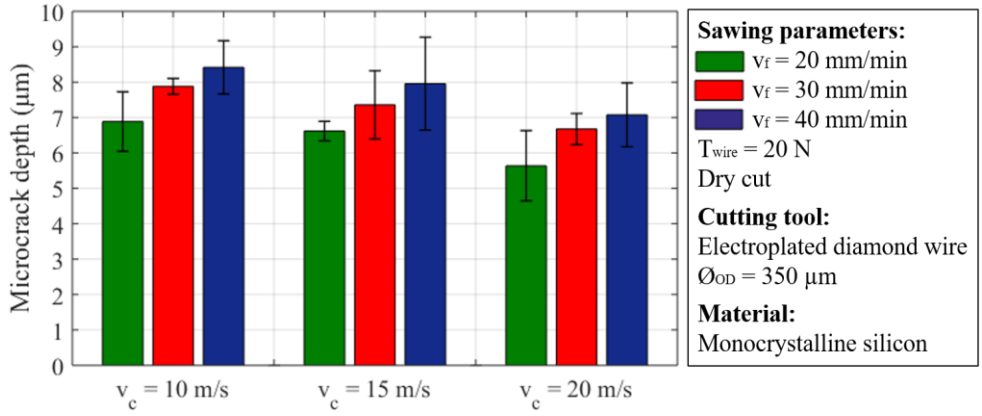

Figure 4. Influence of cutting speed and feed speed of diamond wire sawing on microcrack depth.

On the other hand, microcracks depth presented an average value decrease when v_c was increased from 10→15→20 m/s. Depth microcrack reduction is attributed to the higher diamond grit engagement frequency that promotes decrease of average h_{cu}, which causes less microcracks initiation and propagation. Möller (2015) e Liu *et al.* (2017) add that the reduction is related to smaller sawing force magnitude, since pressure between diamond grains abrasives and mono-Si surface is smaller when v_c is increased.

According to ANOVA results (see Tab. 2), both sawing parameters, feed speed (p-value = 0.00529) and wire cutting speed (p-value = 0.01306), showed significant effect on microcrack depth damage for a confidence level of $\alpha = 0.05$. Increasing v_f from 20 to 40 mm/min enlarged microcrack depth value in +1.44 µm, which causes a +22% increase. Changing v_c from 10 to 20 m/s, microcrack depth decreased the average value in –1.27 µm, leading to a reduction of -16%.

Table 2. ANOVA results for 3^2 full factorial design of experiment for microcrack depth.

Factor	Effect (µm)	Percent (%)	p-value
v_f	+ 1.44	+ 22%	0.00529
v_c	− 1.27	− 16%	0.01306

3.2 Surface roughness

In Fig. 5, it is shown a SEM micrograph of a monocrystalline silicon sawn surface. In general, one can observe that several craters and pittings, as well as parallel and oriented grooves or scratching, compose the surface. Regarding craters and pittings, damage is produced mainly due to the mono-Si brittle behavior when it is subjected to a higher diamond grits penetration, leading to fragile fracture, thus craters formation. On the other hand, ductile regime creates grooves, which follow wire cutting movement direction, suggesting plastic deformation during chip formation. In this sense,

grooves presence is a strong indicative that material was removed in the ductile regime due to the smaller diamond grits penetration depth on mono-Si surface.

Concerning the sawing parameters, it was observed that v_f increase (20→30→40 mm/min) resulted in higher fragile fracture amount in form of craters and pittings, since v_f rise led to higher diamond grit penetration depth. Elevating v_c (10→15→20 m/s), the sawn surface presented a fragile fracture decrease, exhibiting free-damage regions corresponding to grooves, also known as saw marks. The v_c increase promotes higher diamond grit engagement frequency, decreasing diamond grits penetration depth and allowing surface formation in ductile regime.

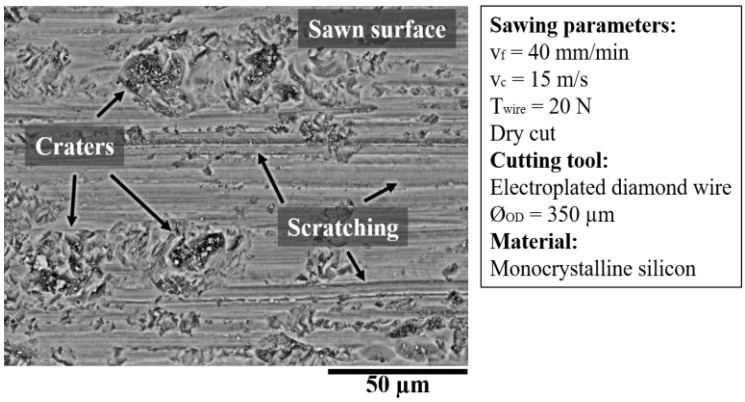

Figure 5. Subsurface microcrack damage of monocrystalline silicon cut by diamond wire sawing.

Surface roughness R_z parameter of monocrystalline silicon wafer sawn was evaluated. Figure 6 shows R_z parameter behavior for the sawing parameters modification (feed speed and wire cutting speed). As seen in Fig. 6, roughness surface R_z parameter increased when v_f was modified from 20 to 40 mm/min. Klocke (2009) attributes surface roughness rise to the higher diamond grit penetration depth. It results in kinematic cutting edges $h_{cu} > h_{cu,crit}$, which promotes craters and pittings formation in the sawn surface due to the mono-Si fragile behavior. Furthermore, v_f increase (20→30→40 mm/min) leads to higher material removal rate, which also contributes to surface roughness growth.

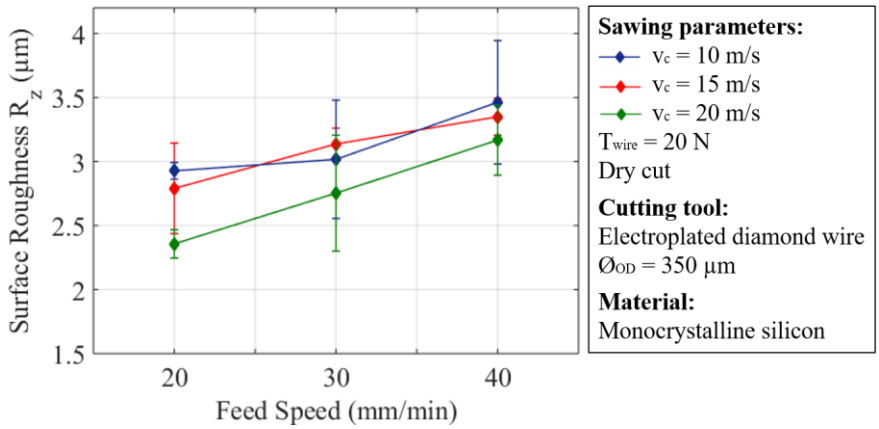

Figure 6. Surface roughness R_z parameter of sawn surface.

At the same time, it was observed that surface roughness decreased when wire cutting speed (v_c) increase from 10→15→20 m/s. According to Costa *et al*. (2019), v_c increase results in surface formation with less craters and pittings and more free-damage grooves. Such behavior is attributed to the higher wire cutting speed, which promotes lower undeformed chip thickness and occasions lower sawing force on each diamond grit. Therefore, sawn surface presents material removal mechanism predominance in the ductile regime when v_c varied from 10 to 20 m/s.

ANOVA results for surface roughness under several sawing parameters is shown in Tab. 3. For this case, both sawing parameters, feed speed (p-value = 0.00184) and wire cutting speed (p-value = 0.04156) showed significant effect for a confidence level of $\alpha = 0.05$. When v_f was raised from 20 to 40 mm/min, surface roughness R_z value increased by + 23.6%. In contrast, for a wire cutting speed change from 10 to 20 m/s, surface roughness R_z parameter exhibited a – 10.7% decrease.

Table 3. ANOVA results for 3^2 full factorial design of experiment for surface roughness.

Factor	Effect (µm)	Percent (%)	p-value
v_f	+ 0.64	+ 24%	0.00184
v_c	− 0.33	− 11%	0.04156

3.3 Relationship between microcrack depth and surface roughness

According to the material removal mechanism, kinematic cutting edge (N_{kin}) action produces a surface containing fragile fractures such as surface damage in form of craters and pittings. According Hed *et al*. (1988), this kind of surface damage results in higher peak-to-valley (p-v) and can be inferred from R_z parameter. Surface roughness R_z parameter is considered an important indicative of N_{kin} maximum penetration depth. Fracture theory reported that penetration depth and surface roughness R_z parameter exhibits a proportional relationship to subsurface damage.

Correspondingly, it is shown in Fig. 7 the relation between subsurface microcrack depth and surface roughness in terms of R_z parameter. Figure 7 shows there is a linear correlation between microcracks depth and surface roughness with a correlation coefficient of $R^2 = 0.847$. Based on R_z parameter, one can state that surface formation occurred by fragile fracture, where cutting edge penetration depth promoted craters formation on the machined surface and caused the surface roughness R_z parameter increase. Craters presence on the sawn surface indicates there was microcrack formation and propagation into the subsurface.

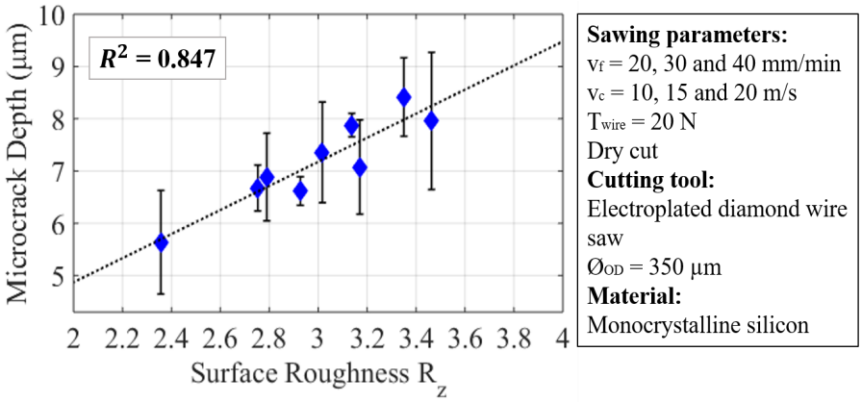

Figure 7. Relation between microcrack depth and surface roughness (R_z).

Furthermore, there is strong evidence that the high kinematic cutting edge penetration depth led to $h_{cu} > h_{cu,crit}$, which allowed microcrack propagation to a larger depth into the subsurface. In other words, when diamond grits penetrate the workpiece, silicon chips are formed mainly through fragile fracture. When the material removal mechanism occurs in brittle regime, it leads to residual damage formation and it extends within the surface. To easily understand microcrack formation from a profile surface, Fig. 8 shows a schematic cross section representation of material removal mechanism for brittle material machining; in this case, for mono-Si diamond wire sawing.

Figure 8a shows a monocrystalline silicon sawn surface profile, where one can observe many peaks and valleys. Considering peaks and valleys as craters formed by the higher penetration depth of diamond grit that causes microcrack formation, Fig. 8b shows a microcrack formation and propagation scheme based in this profile.

As seen in Fig. 8b, N_{kin} action produces tensile and compression stress in monocrystalline silicon. Initially, first contact between diamond grits and workpiece produces elastic deformation by the undeformed chip thickness, which forms a stress zone (tensile or compression). When tensile stress is higher than compression stress, as described by Hertz law, lateral and median microcracks initiates beneath the plastic zone as result of diamond grit and workpiece contact. Then (see Fig. 8c), when material reaches fracture toughness, median microcracks are created. With normal force per grain intensification, the microcrack tends to penetrate deeper into the subsurface. However, median microcracks that penetrate the subsurface remain as residual damage in mono-Si wafer. From a median microcrack depth, one can find an equivalent R_z parameter, as seen in the correlation graphic in Fig. 7.

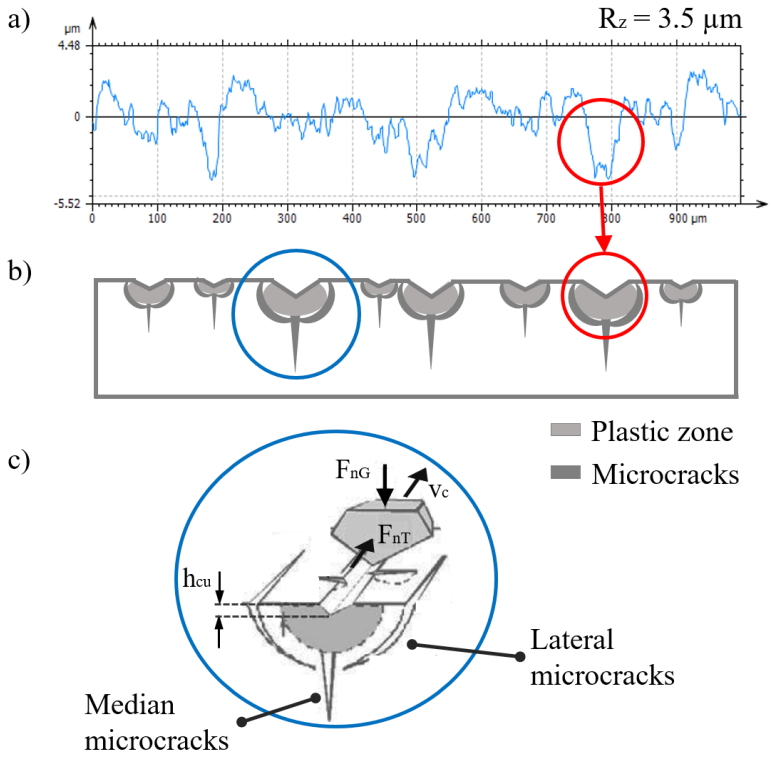

Figure 8. Microcrack formation schematic of a) sawn surface profile; b) material removal mechanism based on sawn surface; c) diamond grit for brittle materials action (Adapted from KLOCKE, 2009).

After diamond grits unload, lateral microcracks emerge to the surface, which cause material removal by microcrack propagation. This leads to shell-shaped or flake-shaped chipping, resulting in craters and pitting on the sawn surface. Chip thickness and width can be larger than the theoretically achievable through overlapping, exhibiting a surface profile with lots of peaks and valleys, as seen in Fig. 8a.

Results obtained in this investigation represent behavior between microcrack depth and surface roughness R_z parameter similar to the one observed by Gao *et al.* (2009). However, higher wire cutting speed (v_c) used in this investigation induced lower subsurface microcracks depth and R_z values.

4. CONCLUSIONS

In this paper, wire cutting speed and feed speed influence on subsurface microcrack formation in monocrystalline silicon cut by diamond wire sawing was evaluated. Sawn mono-Si subsurface was analyzed by bevel-polishing and SEM. Microcrack depth progression under v_c e v_f variation was discussed.

Based on results obtained in this investigation, it can be concluded that:

i. Both sawing parameters exhibited significant influence on microcrack formation. Increasing v_f, substantial microcracks depth rise occurred (around of –22%) due to the higher cutting edge depth of cut. On the other hand, for wire cutting speed v_c increase, microcracks depth was reduced around of –16%, because of the N_{kin} higher engagement frequency, leading to smaller undeformed chip thickness.

ii. Similarly, for surface roughness, both sawing parameters presented significant influence on R_z parameter. For feed speed change, R_z parameter increased around +24%. In contrast, v_c growth resulted in an approximately –11% decrease of R_z parameter. Surface roughness behavior was attributed to the surface characteristic that exhibited craters and pittings.

iii. It was observed a linear correlation ($R^2 = 0.847$) between microcrack depth and R_z parameter surface roughness. According to the results, the R_z parameter increase occurred because of a larger undeformed chip thickness, which resulted in a critical value extrapolation and microcracks formation and propagation. Hence, microcracks also presented larger penetration depth into the subsurface with R_z parameter rise.

A fundamental explanation about microcrack formation based on surface roughness R_z parameter has been done. Peaks and valleys from the profile surface were considered as craters on the sawn surface and a microcrack formation

and propagation scheme was shown. Diamond grit higher penetration depth was recognized as the main reason for microcrack formation in monocrystalline silicon when sawn with diamond wire saw.

5. ACKNOWLEDGEMENTS

The authors would like to thank CAPES (Coordenação de Aperfeiçoamento de Pessoal de Nível Superior) and CNPq (Conselho Nacional de Desenvolvimento Científico e Tecnológico) for financial support to the research; Saint-Gobain Abrasives for supplying the electroplated diamond wire saw; and Swiss Federal Institute of Technology Zurich – ETH for providing monocrystalline silicon specimen.

6. REFERENCES

Bidiville, A.; Wasmer, K.; Van Der Meer, M.; Ballif, C. “Wire-sawing processes: parametrical study and modeling”. *Solar Energy Materials & Solar Cells*, Vol. 132, pp. 392-402, 2015.

Bifano, T. G.; Dow, T. A.; Scattergood, R. O. “Ductile-regime grinding: a new technology for machining brittle materials” *Journal of Engineering for Industry*, Vol. 113, No. 2, pp. 184, 1991.

Costa, E C.; Souza, R. D.; Knoblauch, R.; Weingaertner, W. L.; Xavier, F. A.; Wegener, K. “Corte de silício monocristalino com serra de fio diamantado contínuo”. Anais do 10º Congresso Nacional de Engenharia Mecânica, Salvador – BA, Brasil, pp. 1-7, 2018.

Costa, E C.; Santos, C. P.; Knoblauch, R.; Xavier, F. A.; Weingaertner, W. L. “Análise da superfície do silício monocristalino obtida pelo corte com fio diamantado contínuo”. Anais do 10º Congresso Brasileiro de Engenharia de Fabricação, São Carlos – SP, Brasil, pp. 1-6, 2019.

Gao, Y.; Ge, P.; Liu, T. “Experiment study on electroplated diamond wire saw slicing single-crystal silicon”. *Materials Science in Semiconductor Processing*, Vol. 56, pp. 106–114, 2016.

Gao, Y.; Ge, P.; Li, S. “Investigation of subsurface damage depth of single-crystal silicon in electroplated wire saw slicing”. *Key Engineering Materials*, Vol. 416, pp. 306–310, 2009.

Knoblauch, R. “Continous sawing of monocrystalline silicon with welded diamond wires”. Thesis. Programa de Pós-Graduação em Engenharia Mecânica – UFSC, 2019.

Knoblauch, R.; Costa, J. V. M. T.; Weingaertner, W. L.; Xavier, F. A. Wegener, K. “Endless diamond wire saw for monocrystalline silicon cutting”. *In Proceeding of the 59th Ilmenau Scientific Colloquium*, 2017a, Ilmenau – Germany.

Knoblauch, R.; Silveira, C. A.; Campos, J. E. S.; Weingaertner, W. L.; Xavier, F. A.; Wegener, K. “Test rig for welding diamond wires into a loop”. *In Proceeding of the 5th Int. Conf. Adv. Civil, Struct. Mech. Eng*., 2017b, Zurich – Switzerland.

Klocke, F. “Manufacturing Processes 2: Grinding, Honing, Lapping”. Editor Springer, pp. 452, 2009.

Lawn, B.; Wilshaw, R. “Indentation fracture: principles and applications”. *Journal of Materials Science*, Vol. 10, No. 6, pp. 1049–1081, 1975.

Liu, T.; Ge, P.; Bi, W.; Gao, Y. “Subsurface crack damage in silicon wafers induced by resin bonded diamond wire sawing”. *Materials Science in Semiconductor Processing*, Vol. 57, pp. 147–156, 2017.

Möller, H. J. “Wafering Processing”. *Semiconductors and Semimetals*, Vol. 92, pp. 63–109, 2015.

Pahl, G.; Beitz, W.; Feldhusen, J.; Grote, K. –H. “Engineering Design - A Systematic Approach”, Third Edit. Springer, 2007.

Stoeterau, R. L. “Desenvolvimento do protótipo de uma máquina-ferramenta comandada numericamente para usinagem de ultraprecisão com ferramenta de geometria definida”. Thesis. Programa de Pós-Graduação em Engenharia Mecânica – UFSC, 1999.

Tönshoff, H. K.; Karpuschewski, B.; Hartmann, M.; Spengler, C. “Grinding-and-slicing technique as an advanced technology for silicon wafer slicing”. *Machining Science and Technology*, Vol. 1, No. 1, pp. 33–47, 1997.

Wu, H. “Wire sawing technologies: state-of-the-art review”. *Precision Engineering*, Vol. 43, pp. 1–9, 2016.

7. RESPONSIBILITY NOTICE

The authors are the only responsible for the printed material included in this paper.